Energy and Buildings 103 (2015) 1–13

Contents lists available at ScienceDirect

Energy and Buildings

journal homepage: www.elsevier.com/locate/enbuild

Influence of plant coverage on the total green roof energy balance and building energy consumption

Neda Yaghoobian*, Jelena Srebric

Department of Mechanical Engineering, University of Maryland, College Park, MD, USA

ARTICLE INFO

Article history:
Received 8 January 2015
Received in revised form 25 April 2015
Accepted 31 May 2015
Available online 2 June 2015

Keywords:
Building energy simulation
Green roof
Plant coverage
Surface energy balance

ABSTRACT

This study quantifies the influence of green roof plant coverage on the building energy consumption and the substrate energy balance components. The analysis started with the implementation of a green roof model that accounts for the effects of plant coverage into the U.S. Department of Energy (DOE) building energy simulation program, EnergyPlus. Using the DOE reference building models, thirty different cases were simulated considering different green roof plant coverage, building type, and building age for two different climates. The results indicated that the green roof substrate surface temperature decreases with increasing plant coverage. This temperature decrease is primarily due to the decrease in the amount of absorbed solar radiation on the substrate surface and also an increase in the substrate surface evaporation. For the base-case simulation, due to the plant shading effects, the total daily received radiation at the bare-soil surface is 32% (6.2 kWh m^{-2}) higher than that at the fully-covered green roof substrate surface. Furthermore, the annual cooling (heating) load decreases (increases) with the rate of 13 (0.88) kWh m^{-2} of plant coverage area. The aim of this study is to show the importance of considering plant coverage in green roof simulations and building energy demand predictions.

1. Introduction

As the human population grows, many more natural surfaces turn into impervious surfaces to support infrastructure development for the city dwellers [1,2]. Replacing the natural land cover with buildings and impervious surfaces changes the local energy balance due to different radiative and thermal properties of the newly-introduced materials. These modifications create a different microclimate in the urban areas compared to the microclimate in the rural areas. Turning traditional black flat roofs that constitute about 20–25% of the urban surfaces [3] into green roofs is one of the potential solutions to restore some of natural habitats destroyed in the process of developing city infrastructure. Green roofs are one of the oldest and well-known techniques to reduce the negative effects of urbanization and have been recognized as one of the urban heat island (UHI) mitigation strategies [4]. Green roofs can mitigate the effects of impervious surfaces such as storm water runoff [5,6], and higher surface and ambient air temperatures [7,8]. Therefore, green roofs offer multiple benefits to cities from the water and energy flow perspectives. Urban- and building-scale benefits and positive effects of green roofs have been explored in several studies using numerical simulations, field measurements and laboratory experiments [9–16]. In their lifecycle, green roofs are not continuously fully-covered with plants resulting in heterogeneity along the green roof surfaces. Heterogeneity in roughness, shading, and soil moisture content creates nonuniformity in energy and mass transport over green roofs. In practice, to reduce the green roof heterogeneity and to speed plant growth rate at the initial period of a green roof lifecycle, pre-cultivated vegetation mats are used [17]. Therefore, studying the green roof heterogeneity and plant coverage effects on the green roof energy balance and building energy consumption is required to understand the performance of green roofs.

An extensive literature review indicates that despite a long history of valuable studies in the area of green roofs, the effects of the green roof plant coverage (defined as the percentage of the roof area covered with plants to the total green roof area) have not been studies, quantitatively.

Most of the detailed existing green roof models account for the effects of the plant canopy height and density [18–20], but due to the horizontally-homogeneous assumptions, heterogeneity effects along the green roof surfaces are neglected. Heterogeneity in green roof plant coverage is explicitly considered in a recently developed model by Tabares-Velasco and Srebric [14] (hereinafter

* Corresponding author. Current address: Department of Mechanical Engineering, Johns Hopkins University, Baltimore, MD 21218, USA. Tel.: +1 8585396416.
E-mail addresses: neyaghoo@gmail.com (N. Yaghoobian), jsrebric@umd.edu (J. Srebric).

http://dx.doi.org/10.1016/j.enbuild.2015.05.052
0378-7788/

Nomenclature

C_p	specific heat of air, J kg^{-1} K^{-1}
e_{air}	vapor pressure in the air, kPa
e_{soil}	saturated vapor pressure at the soil/substrate temperature, kPa
h_{conv}	convective heat transfer coefficient for plant layer, W m^{-2} K^{-1}
h_{por}	convective heat transfer coefficient for porous media (plants), W m^{-2} K^{-1}
h_{sub}	total convective heat transfer coefficient for green roof substrate, W m^{-2} K^{-1}
k_l	longwave extinction coefficient
k_s	shortwave extinction coefficient
LAI	leaf area index [(leaf area)/(soil surface)]
$LMST$	Local Mean Sidereal Time
LW_{net_Plant}	thermal radiative exchange between the plant layer and the soil surface absorbed by the soil surface, W m^{-2}
LW_{net_Sky}	thermal radiative exchange between the sky and the soil surface absorbed by the soil surface, W m^{-2}
Q_E	substrate surface latent heat flux, W m^{-2}
Q_{E_bare}	substrate latent heat flux of the uncovered portions of the green roofs, W m^{-2}
$Q_{E\_covered}$	substrate latent heat flux of the covered portions of the green roofs, W m^{-2}
Q_G	conductive heat flux through green roof substrate and roof construction, W m^{-2}
Q_S	substrate surface sensible heat flux, W m^{-2}
r_a	aerodynamic resistance to mass transfer, s m^{-1}
r_{sub}	substrate surface resistance to mass transfer
R_s	total shortwave radiation received at the substrate surface, W m^{-2}
SW_{net}	substrate surface net absorbed shortwave radiation, W m^{-2}
T_{plant}	plant temperature, K
T_{sky}	sky temperature, K
VWC	substrate average volumetric water content, m^3 m^{-3}
VWC_{sat}	substrate maximum volumetric water content, m^3 m^{-3}

Greek

γ	psychrometric constant, kPa K^{-1}
δ_f	plant coverage (PC)
ε_g	soil emissivity
ε_p	plant emissivity
ε_s	sky emissivity
ρ	air density, kg m^{-3}
τ_{lw}	longwave transmittance of a plant canopy
τ_{sw}	shortwave transmittance of a plant canopy

GR-TS2012). GR-TS2012 is a physically-based, quasi-steady state heat and mass transfer green roof model that introduced the plant coverage as a percentage of the total green roof area. The aim of the current study is to use a modified version of GR-TS2012 to explore and quantify the effects of plant coverage on the extensive type green roof surface energy balance and further explore its influence on the energy demand in buildings. Therefore, GR-TS2012 was implemented into EnergyPlus, the U.S. Department of Energy (DOE) building energy simulation program [21]. If successfully implemented, this simulation module can enable numerical calculations of green roof plant coverage impacts on the building energy consumption. Therefore, beyond the model implementation, this study validated the module with data from measurements and conducted simulations of thirty different cases considering different green roof plant coverage, building type, and building age for two different climates. Overall, the study deployed a detailed green roof model in a comprehensive way to quantitatively evaluate impacts of the green roof plant coverage on the total green roof energy balance and the thermal performance of a building.

2. Model description

This study uses a quasi-steady state heat and mass transfer green roof model that was developed from data collected in a "Cold Plate" apparatus set in an environment chamber [22]. The detailed description of this model, which in this paper is referred to as GR-TS2012, is available in the literature [14]. This model is fully validated with laboratory and field experimental data including both heat fluxes and surface temperature fields [14,23]. The unique characteristic of this physically-based model is the ability to simulate partially-exposed/partially-covered, including bare-soil and fully-covered green roofs by taking into account the plant coverage percentage. GR-TS2012 was originally implemented in the Engineering Equation Solver (EES) software to solve the heat and mass transfer equations between the sky, plants and substrate. In order to investigate the effects of a green roof plant coverage on building energy performance in this study, GR-TS2012 was integrated into the U.S. Department of Energy (DOE) building energy simulation software, EnergyPlus [21]. EnergyPlus is one of the most advanced building energy simulation models that is supported by DOE for analyzing the energy consumption of buildings. EnergyPlus is a stand-alone building energy simulation model that simulates the hourly energy consumption of a building conditional on user-specified internal loads, building construction, and weather. More information about EnergyPlus can be found in the corresponding DOE publications [24,25]. For implementing GR-TS2012 into EnergyPlus, GR-TS2012 was written in FORTRAN and later in C++ language. In its new format, the energy balance equations for plants, bare soil surface, and substrate surface under the plant layer were solved iteratively for their temperatures by Newton's method. Furthermore, using the plant coverage percentage, the area-averaged soil surface temperature is calculated as the roof surface temperature. The volumetric water content (VWC) in the substrate layer is simulated by the moisture-tracking subroutine of EnergyPlus that accounts for precipitation, irrigation, evapotranspiration, and runoff [20]. Similar to the existing 'Ecoroof' model option in EnergyPlus, in the current model, the user is allowed to specify a green roof layer as the outer layer of a rooftop construction [20]. Besides the 'Ecoroof' inputs that include growing media depth, soil physical and thermal properties, plant canopy density, stomatal resistance, and soil moisture conditions, additional parameters are required for the new green roof model. The new parameters are the plant coverage representing the percentage of green roof area covered with plants, the substrate VWC at field capacity, as well as the shortwave and longwave extinction coefficients [26]. GR-TS2012 requires additional inputs, but they are crucial in accounting for thermal effects of partially covered green roofs.

To verify the implementation of the green roof model into EnergyPlus, the model was tested against field data from a green roof installed on a commercial building roof in Chicago, IL, the same case that was used in the previous field validation study of GR-TS2012 [23]. Recreation of the GR-TS2012 validation study verified that the implemented model into EnergyPlus works as expected.

Table 1
Thicknesses and properties of the roof material layers for the DOE reference buildings in Baltimore, MD. Roof material properties in Phoenix, AZ are the same as the material properties in Baltimore, MD except the material thicknesses provided in parentheses. This table is based on the DOE reference building models [34].

Material layer	Thickness (m)	Conductivity ($W m^{-1} K^{-1}$)	Density ($kg m^{-3}$)	Specific heat ($J kg^{-1} K^{-1}$)
Roof membrane	0.0095	0.16	1121.3	1460
Metal decking	0.0015	45	7680	418.4
IEAD non-res insulation (new const. – retail)	0.125	0.05	265	836.8
IEAD non-res insulation (post-1980 – retail)	0.136 (0.175)[a]	0.05	265	836.8
IEAD non-res insulation (pre-1980 – office)	0.088 (0.074)[a]	0.05	265	836.8
IEAD non-res insulation (pre-1980 – retail)	0.088 (0.074)[a]	0.05	265	836.8

[a] Numbers in parentheses are material thicknesses in Phoenix, AZ.

3. Simulation setup

Energy performance of buildings in response to the green roof plant coverage depends on several factors such as local climate, building use type, building age, as well as the green roof material and the roof assembly underneath the green roof. These factors are considered as the key input parameters for the building energy simulations to enable direct performance comparisons.

3.1. Scenarios for climate, building type, building age, and green roof plant coverage

Thermal performance of green roof assemblies depends on the local climate because the green roof material properties are highly dependent on outdoor environmental conditions [19,27]. A study of the green roof thermal performance showed that the material selection for green roof assemblies is more important in climate zones 4 and 5 than the material selection for buildings located in climate zones 2 and 3 [27]. Based on these finding, the present study used the typical meteorological year (TMY2 [28]) weather data files for Baltimore, Maryland (39.17° north latitude, 76.67° west longitude and 47 m altitude) located in climate zone 4 with mixed-humid climate and Phoenix, Arizona (33.42° north latitude, 112.02° west longitude and 339 m altitude) located in climate zone 2 with hot- to mixed-dry climate to represent different environmental conditions.

The U.S. Department of Energy (DOE) developed commercial reference building models that consist of sixteen building types, and represent approximately two-thirds of the U.S. commercial building stock. These model buildings feature realistic building characteristics and construction practices that provide a consistent baseline for comparison of building energy simulations [29]. Among these building types, this study used one-story buildings that include small office and stand-alone retail buildings. Previous studies showed that office buildings and retail stores are the commercial building types with the largest amount of energy use in the U.S. [30].

The energy use in single-story buildings strongly depends on the roof insulation that could also limit the energy saving benefits of green roofs for buildings with well-insulated roofs. Older buildings with poorly insulated roofs are expected to benefit more from green roofs than newer-built buildings with a higher level of insulation [11,31–33]. To address the effects of green roof plant coverage on buildings with different levels of insulation, the DOE commercial reference building models for all three categories of new-construction, post-1980, and pre-1980 buildings [34] were used in this study. The differences among these buildings are reflected in the insulation levels, infiltration rates, lighting intensities, as well as HVAC equipment types and efficiencies. The new-construction models comply with the minimum requirements of ANSI/ASHRAE/IESNA Standard 90.1-2004 [35], the post-1980 models meet the minimum requirements of Standard 90.1-1989 [36], and pre-1980 models are based on previous standards and other studies of construction practices [29].

Considering that green roof plants take several months to become fully established, and the roofs may not stay fully covered during their lifespans, it is desirable to study a range of green roof growth coverage rates from bare-soil to fully-covered roofs. For this reason, the plant coverage (δ_f) of 0% (bare soil), 25%, 50%, 75%, and 100% (fully covered with plants) was considered in this study.

3.2. Conventional and green roof assembly materials

As stated in the previous section, this study examined the three categories of new-construction, post-1980, and pre-1980 buildings of small office and stand-alone retail buildings from the DOE commercial reference building models [34] in Baltimore, MD and Phoenix, AZ. Energy performance of these buildings were modeled with and without an additional set of layers for the green roof. Based on the DOE commercial reference buildings, roofs of the stand-alone retail buildings in all three categories of new-construction, pre- and post-1980 buildings, plus pre-1980 small office buildings are the same and of the type of 'Insulation Entirely Above Deck (IEAD) non-residential' roof, but the thickness of their insulation layers is different. In new-construction and post-1980 small office buildings, roofs are of the type of 'attic non-residential' roofs. The building roof types are the same for both Baltimore and Phoenix. IEAD non-residential roofs consist of three layers including the roof membrane, IEAD non-residential roof insulation, and metal decking. Attic non-residential roofs consist of two layers including the roof membrane, and metal decking. Roof types and physical characteristics of their material layers are provided in Table 1. Sketch of the layers of the IEAD non-residential, attic non-residential, and green roofs are presented in Fig. A1 of Appendix.

For a set of realistic simulations, the construction assembly of green roof is defined based on an extensive type green roof located in Chicago, Illinois used in the previous validation study of GRTS2012 [23], and also in a green roof material study [27]. The green roof material layers, which are placed over the conventional roofs, and their physical characteristics are presented in Table 2. Table 3

Table 2
The green roof material layers from top to bottom [10,23,27,37–40].

Layer name	Layer type	Thickness (m)	Thermal conductivity ($W m^{-1} K^{-1}$)	Density ($kg m^{-3}$)	Specific heat ($J kg^{-1} K^{-1}$)
Substrate	Expanded clay	0.075	0.32	682	1065
Filter membrane	Two layers of polypropylene fabric layers	0.002	0.137	900	1926
Drainage layer	Recycled closed cell polystyrene	0.025	0.033	25	1170
Waterproof membrane	PVC	0.002	0.19	1370	1046

Table 3
Information of the green roof soil and plant canopy [14,23,27].

Plant type	Mixed sedum species
Plant albedo	0.11
Soil albedo	0.12
Minimum stomatal resistance	700 s m^{-1}
Leaf area index (*LAI*)	2.5 (m^2 m^{-2})
Shortwave extinction coefficient (k_s)	0.7
Longwave extinction coefficient (k_l)	0.83
Leaf emissivity	0.98
Soil emissivity	0.95
Substrate maximum volumetric water content (VWC_{sat})	0.55 (m^3 m^{-3})
Substrate volumetric water content at field capacity	0.33 (m^3 m^{-3})

includes the green roof soil and plant canopy data. The green roof characteristics were kept constant in all of the simulations.

4. Results and discussion

To study the importance of the green roof plant coverage, it is necessary to explore its effects on the green roof energy balance components individually, and on the substrate surface temperature as a whole. In addition, studying the annual and diurnal variations of building energy use with respect to the change in the green roof plant coverage in different buildings and climates illuminates the importance of this parameter in building energy simulations. For these reasons, the influence of plant coverage on both the total green roof energy balance and building energy consumption were examined in the simulations. Since the energy balance analysis of snow layers is not considered in the current versions of GR-TS2012 and EnergyPlus, the diurnal results of this study are restricted to the summertime. Unless stated otherwise, all the diurnal results are monthly averages for the typical meteorological month of July in Phoenix with average wind speed of 3.6 m s^{-1}, average relative humidity of 35%, average air temperature of 33 °C, and low cloud coverage in average. July month is selected to be representative of midsummer. The pre-1980 small office building is considered as the base-case simulation.

4.1. Importance of considering the green roof plant coverage in green roof simulations

To calculate a green roof substrate surface temperature and investigate its effects on building energy use, it is necessary to understand the energy balance for the green roof. In general, the temperature of the green roof substrate surface is not uniform and varies across the green roof depending primarily on the amount of plants covering the soil surface. In the current green roof model implemented in EnergyPlus, the green roof substrate surface temperature at each time step is computed as an area-averaged temperature based on the bare-soil and the covered-soil surface temperatures. Similarly, the heat fluxes at the green roof are area-averaged heat fluxes of both the bare and vegetated roof areas. The *average* substrate surface temperature represents the roof surface temperature used in the building energy simulations. The importance of plant coverage for green roof simulations is investigated by comparing the results of the substrate surface energy balance for the bare-soil and fully-covered green roofs. The following equation shows the energy balance for a green roof soil surface:

$$SW_{net} + LW_{net\_Sky} + LW_{net\_Plant} = Q_S + Q_E + Q_G \quad (1)$$

where SW_{net} is the net absorbed shortwave radiation by the substrate surface, LW_{net_Sky} is the net exchange of longwave radiation between the sky and the soil absorbed by the soil surface, LW_{net_Plant} is the net exchange of longwave radiation between the plant layer and the soil surface absorbed by the soil surface that is zero for a bare-soil roof, Q_S and Q_E are the sensible and latent convective heat fluxes over the substrate surface, and Q_G is the conductive heat flux through the substrate and roof construction layers. Unlike the energy balance components for the bare-soil roof, the energy balance components for the fully-covered green roof are affected by the plant layer.

4.1.1. Plant coverage effects on the total received radiation at the substrate surface

The following equations represent the total amount of radiation (Rad_{Total}) received at the surface of bare-soil, fully-covered, and partially covered green roofs in GR-TS2012 [14]:

$$Rad_{Total\_bare} = R_s + \varepsilon_s \sigma T_{sky}^4 \quad (2)$$

$$Rad_{Total\_covered} = \tau_{sw} R_s + \tau_{lw} \varepsilon_s \sigma T_{sky}^4 + (1 - \tau_{lw}) \frac{\varepsilon_p \varepsilon_g}{\varepsilon_p + \varepsilon_g - \varepsilon_p \varepsilon_g} \sigma T_{plant}^4 \quad (3)$$

$$Rad_{Total\_partial} = \delta_f \cdot Rad_{Total\_covered} + \left(1 - \delta_f\right) \cdot Rad_{Total\_bare} \quad (4)$$

where R_s is the total shortwave radiation received at the substrate surface, ε_s (ε_p) and T_{sky} (T_{plant}) are the sky (plant) emissivity and temperature, ε_g is the soil emissivity, τ_{sw} and τ_{lw} are the shortwave and longwave transmittance of a canopy, σ is the Stefan–Boltzmann constant, and δ_f is the plant coverage ratio. In the simulations, R_s and T_{sky} are hourly inputs from the EnergyPlus TMY2 weather data file for Baltimore and Phoenix.

The amount of shortwave radiation received at the substrate surface underneath the plant layer is the sum of the un-intercepted radiation and the radiation that is transmitted and/or reflected by the canopy leaves. Furthermore, the longwave radiation is the sum of un-intercepted sky thermal radiation and the radiation emitted by the plant layer. The shortwave transmittance of a canopy (τ_{sw}) is $e^{-k_s LAI}$ [14], where k_s is the extinction coefficient and *LAI* is the leaf area index. The transmittance of thermal radiation (τ_{lw}) is the radiation that is not intercepted by any leaf and is calculated similar to τ_{sw}, but with a different extinction coefficient (k_l) [14]. For the base-case, Fig. 1 compares monthly averaged diurnal results of the received shortwave, longwave, and total incoming radiation at the soil surface of green roofs with different plant coverage (PC) for the month of July in Phoenix. The differences in the received radiation for the bare-soil and fully-covered green roofs are significant as shown in Fig. 1.

Due to the plant shading effects, the received shortwave radiation at the substrate surface of a fully-covered green roof is much smaller than that over the bare-soil with the total difference of 83% as shown in Fig. 1a. This amount is highly dependent on the plant density of the canopy that, in the green roof model, is accounted through the *LAI* variable, and the canopy shortwave extinction coefficient. Density of the plant canopy depends on several factors (e.g. plant type, weather condition, water availability) and is variable throughout a year and at different geographical locations. For the same reason, the amount of received sky thermal radiation is smaller at the soil surface covered by the plants. However, since the plant layer and the underneath soil surface have thermal interactions, the total amount of incoming longwave radiation at the soil surface covered by the plants is 19% larger than the amount of longwave radiation received at the bare-soil surface (Fig. 1b). Furthermore, Fig. 1c reveals that the total amount of radiation over 24 h period for a bare-soil roof is 19.4 kWh m^{-2} that is 6.2 kWh m^{-2} larger than the total radiation received at the substrate surface of a fully-covered green roof. In another word, the daily integrated value of the received total radiation at the substrate surface of a

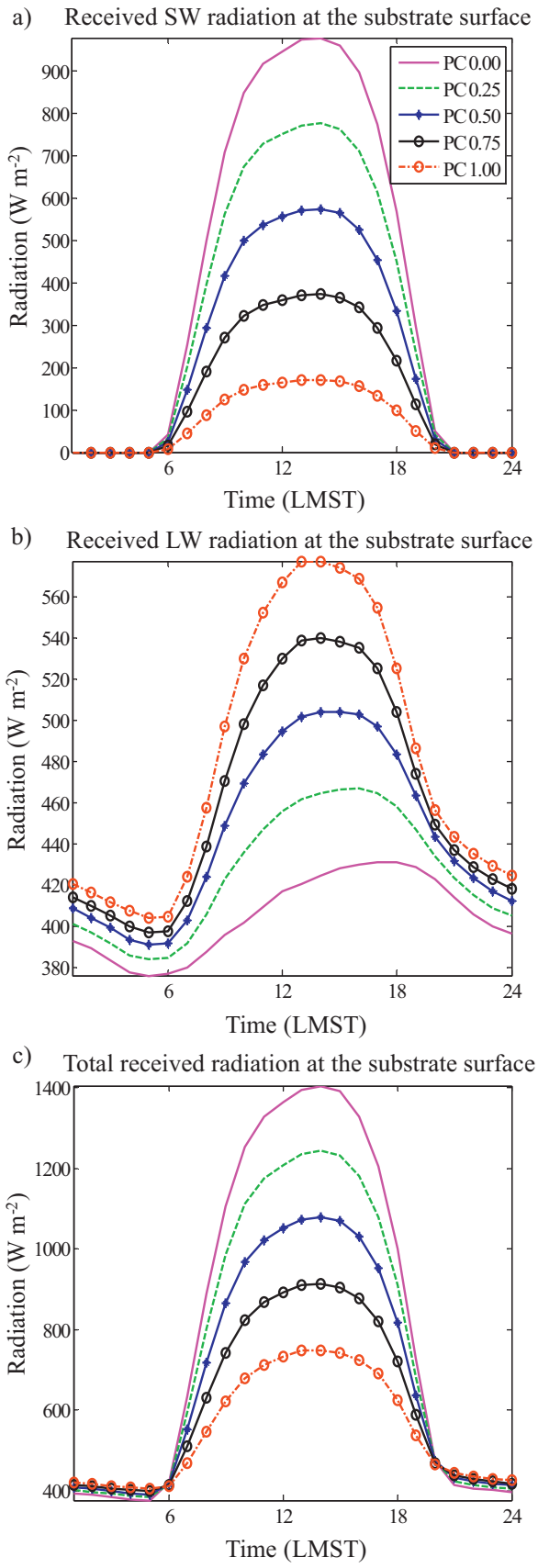

Fig. 1. Monthly averaged diurnal results of (a) shortwave, (b) longwave, and (c) total radiation received at the green roof substrate surface with the plant coverage (PC) of 0.0, 0.25, 0.5, 0.75, and 1.0 for the month of July in Phoenix, AZ for the base-case simulation. *LMST* stands for the Local Mean Sidereal Time.

bare-soil roof can have up to 32% error, if the plant coverage effects are not considered in the green roof simulations.

4.1.2. Plant coverage effects on the substrate surface convective heat fluxes

The amounts of plant coverage affect sensible and latent heat fluxes over the substrate surfaces of green roofs. In general, existence of a plant layer makes the substrate convective heat transfer more complex, and in simulations, this complexity reflects on the convective heat transfer coefficient. The following equation represents the general form of the sensible heat transfer coefficient over the soil surface of a fully-covered green roof (h_{sub}) in GR-TS2012 [14]:

$$h_{sub} = h_{por} \cdot h_{conv} / \left(h_{por} + h_{conv}\right) \tag{5}$$

In Eq. (5), h_{conv} is a function of the Nusselt number for the forced, mixed, and natural convection on a flat surface and h_{por} accounts for the sheltering and roughness effects of the plant layer. The details of the h_{sub} calculation can be found in [14].

Fig. 2a shows monthly averaged diurnal cycles of the substrate sensible heat transfer coefficients for green roofs of the base-case with different plant coverage. Fig. 2b shows wind speed at the roof height for the month of July in Phoenix. Fig. 2 indicates that the soil sensible heat transfer coefficients significantly decrease with increasing plant coverage, and they follow the trend of the wind speed at the roof height. The sensible heat transfer is a complex dynamic phenomena that depends on several parameters, but the correlation between this coefficient and wind speed shown in Fig. 2 indicates that a reduced wind speed in the foliage layer is the main reason for the smaller convective heat transfer coefficients over the covered green roofs.

Generally, the water vapor removal from the soil surface is subjected to the vapor pressure difference of the air layer and the soil surface, as well as the air speed over the soil surface and within the plant canopy. In GR-TS2012, the evaporation rate from the soil surface (Q_E) is calculated using the following equation [14]:

$$Q_E = \frac{\rho C_p}{\gamma(r_{sub} + r_a)}(e_{soil} - e_{air}) \tag{6}$$

where ρ and C_p are the density and specific heat of air, γ is the psychrometric constant, e_{soil} is the saturated vapor pressure at the soil temperature, e_{air} is the vapor pressure in the air, r_a is the aerodynamic resistance to mass transfer that accounts for the sheltering and roughness effects of the plant layer. r_{sub} $(= 34.5(\frac{VWC}{VWC_{sat}})^{-3.3})$ is the substrate surface resistance to mass transfer that depends on the ratio of the average substrate volumetric water content (VWC) and the substrate volumetric water content at saturation (VWC_{sat}); specifically, the drier the soil, the larger the resistance to water vapor.

To understand the plant coverage effects on the complex and dynamic process of the substrate evaporation, Fig. 3a and b respectively show the substrate surface latent heat fluxes from the areas of green roofs with and without plants. Furthermore, Fig. 3c shows the area-averaged substrate latent heat fluxes for green roofs with different plant coverage. Fig. 3d represents the near surface moisture content for the base-case that is dynamically simulated by the moisture-tracking subroutine of EnergyPlus.

Fig. 3b shows that, similar to the substrate latent heat flux of the covered portions of the green roofs, $Q_{E\_covered}$ (Fig. 3a), the substrate latent heat flux of the uncovered portions of the green roofs, Q_{E_bare}, increases with increasing plant coverage percentage. That is because the energy balance for the bare and covered portions of a green roof are not independent and they interact dynamically. The elevated soil surface latent heat fluxes with increasing plant coverage are consistent with the fact that the average

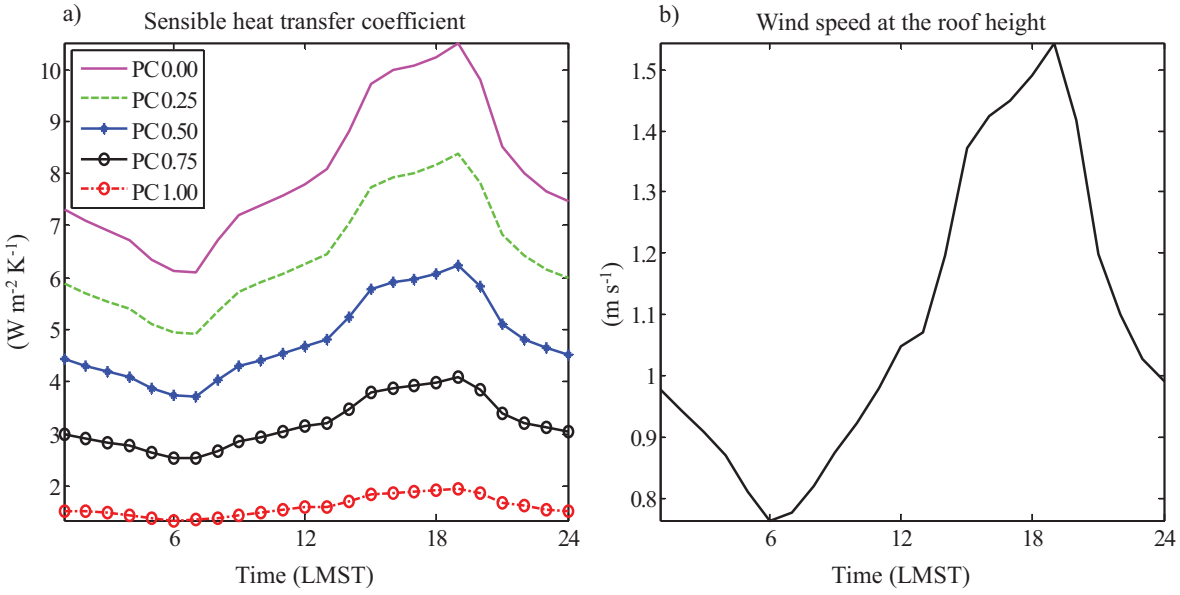

Fig. 2. Monthly averaged diurnal results including (a) sensible heat transfer coefficients for green roofs with plant coverage (PC) of 0.0, 0.25, 0.5, 0.75, and 1.0, and (b) wind speeds at the roof height for the month of July in Phoenix, AZ for the base-case simulation.

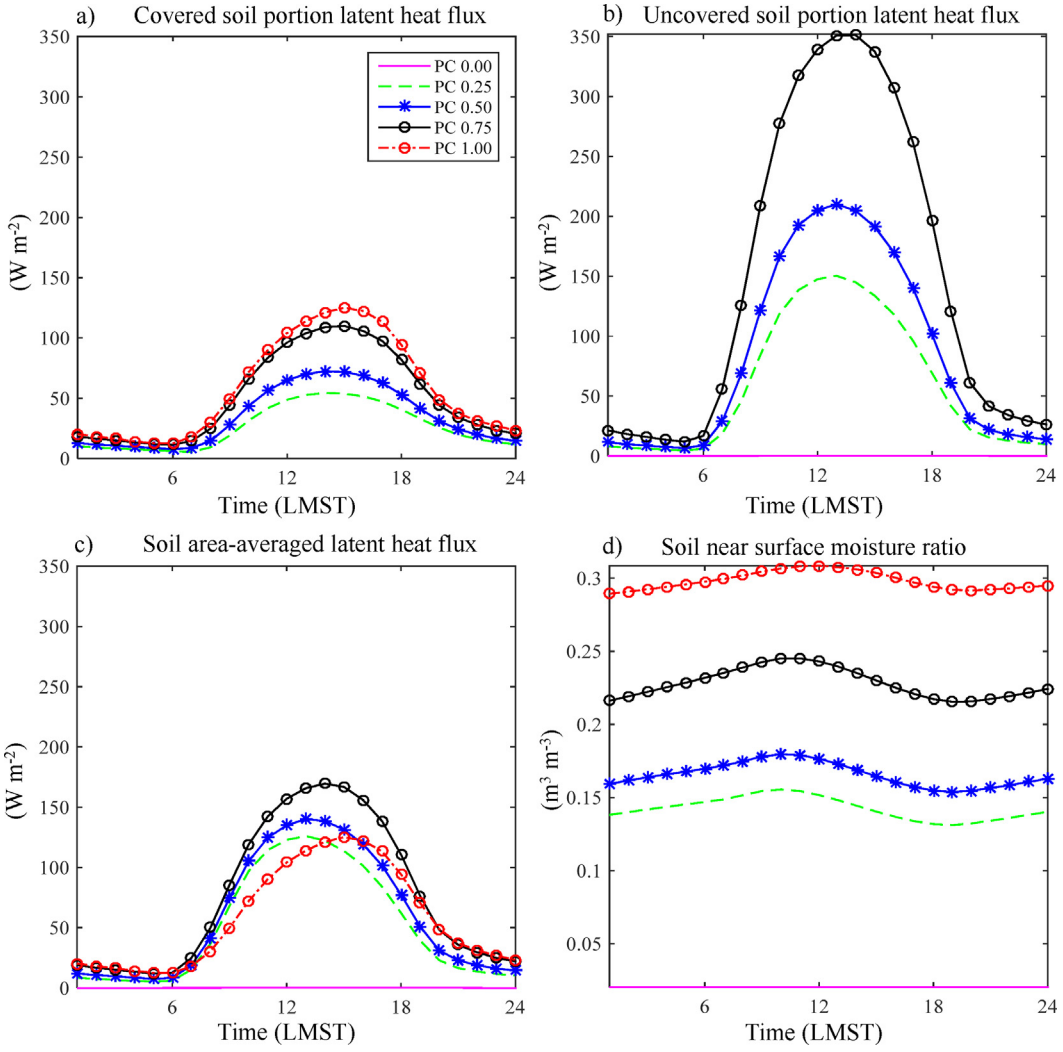

Fig. 3. Monthly averaged diurnal results including (a) covered soil, (b) uncovered soil, and (c) soil average latent heat fluxes, and (d) moisture content near the soil surface of green roofs with plant coverage (PC) of 0.0, 0.25, 0.5, 0.75, and 1.0 for the month of July in Phoenix, AZ for the base-case simulation.

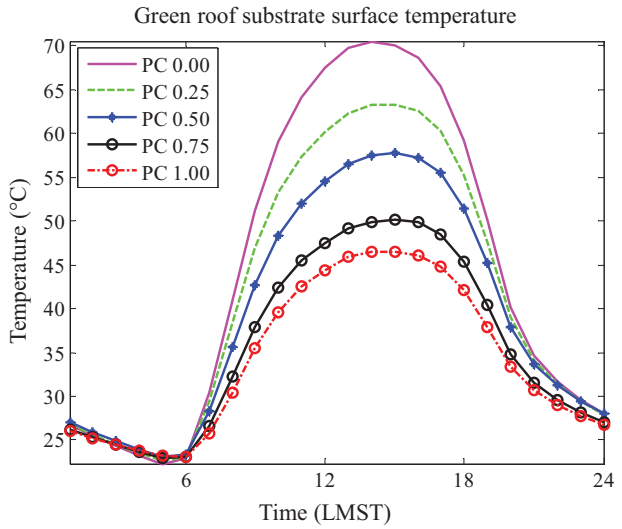

Fig. 4. Monthly averaged diurnal cycle of substrate surface temperatures for green roofs with plant coverage (PC) of 0.0, 0.25, 0.5, 0.75, and 1.0 for the month of July in Phoenix, AZ for the base-case simulation.

near-surface moisture level with larger plant coverage is larger (Fig. 3d). However, comparing Fig. 3a and b indicates that the evaporation from the uncovered portions of the green roofs is larger than that over the covered portions by a factor of 3. That is because over the bare soils the air speed is larger and thus the aerodynamic resistance to mass transfer is smaller. That explains the behavior of the area-averaged substrate latent heat flux that is defined by $Q_{E\_covered} + (1 - \delta_f)Q_{E\_bare}$ for the green roofs with different plant coverage in Fig. 3c. This figure shows that the latent heat flux over the fully-covered green roof in the base-case simulation is smaller than that over the 75%- and 50%-covered green roofs, and its maximum is similar to that of the 25%-covered green roof, except for the time lag of few hours.

4.1.3. Plant coverage effects on the conductive heat flux

Conduction is a complex process that depends on the soil material properties, surface and deep-soil temperatures, as well as the soil moisture content. A larger amount of moisture in the soil media increases the soil conductivity. Thus, in response to the soil moisture content, the average soil thermal properties vary. Convective process via water movement within the soil layers is small and negligible. As Fig. 3d shows, the amount of soil moisture varies with plant coverage. However, due to the use of the EnergyPlus conduction model (Conduction Transfer Functions; CTFs), these effects are not considered in the current green roof study, meaning that the substrate thermal properties do not vary in response to the soil moisture content. The reason is that the CTFs coefficients for each type of material are determined only once at the beginning of the simulations and they remain unchanged during the simulations. Variable thermal properties of the materials cause numerical instabilities in the CTF simulation method. Therefore, in the new green roof simulation module in EnergyPlus, the soil conduction response to the plant coverage only depends on the substrate surface temperature. Previous studies showed that seasonal and hourly variations of thermal conductivity have a relatively small impact on the overall thermal performance of a green roof when compared to the effects of radiation and evapotranspiration [22,41]. Moreover, several validation studies indicated that GR-TS2012 is accurate even with the constant soil thermal properties [14,23].

4.1.4. Green roof substrate surface temperatures

Fig. 4 compares substrate surface temperatures of green roofs with different plant coverage for the pre-1980 small office building (the base-case simulation) for a typical July day in Phoenix. This figure shows that the soil surface temperature decreases with increasing plant coverage. That is primarily due to the larger amount of received shortwave radiation and consequently the larger amount of total absorbed shortwave radiation at the substrate surfaces of the less covered green roofs. The smaller near surface moisture content in less covered green roofs and their smaller amounts of latent heat flux are the second important reason for their higher surface temperatures.

Based on Fig. 4, for the base-case, the substrate surface temperature difference between the fully-covered and bare-soil roofs reaches 24 °C at 1400 LMST*LMST*. In another word, green roof models considering only the fully-covered green roof surfaces may predict the substrate surface temperature of a bare-soil roof with an error of up to 34%.

4.2. Building energy consumption

Fig. 5 shows annual thermal loads of new-construction, post-, and pre-1980 buildings with respect to change in green roof plant coverage for the two building types, small office and stand-alone retail, in Baltimore and Phoenix. This figure shows that for all cases the annual cooling loads decrease with the increasing plant coverage, and the annual heating loads increase with the increasing plat coverage. However, the decrease in annual cooling demands overweigh the increase in annual heating demands in all cases. Furthermore, due to the weaker roof insulation, thermal loads of the buildings built before 1980, are more sensitive to the change in the plant coverage (Fig. 5e and f). In all simulated cases, the annual cooling loads of the buildings in Phoenix are larger and more sensitive to the plant coverage than the annual cooling loads of the buildings in Baltimore. In addition, the annual heating loads in Baltimore are larger than the annual heating loads in Phoenix. For the pre- and post-1980 buildings, the sensitivity of annual cooling loads to the plant coverage in office buildings is larger than the sensitivity in retail buildings. However, in the new-construction building, this annual cooling load sensitivity to the plant coverage is larger for the retail buildings compared to the sensitivity for the office buildings. These trends are related to the relative dependence of thermal loads on the building type and age which are reflected in the roof heat gains/losses, internal heat gains, and infiltration rates.

Aside from the plant coverage effects on building energy use, Fig. 5 also reveals that the pre-1980 buildings require the highest amount of heating and cooling energy, followed by the requirements for the post-1980 buildings and new-constructions. The energy demand differences between these buildings are related to their differences in insulation levels, lighting intensities, and infiltration rates.

4.2.1. Effects of the plant coverage

Fig. 5 indicates that for buildings of any age and type, a change in the annual thermal loads with respect to a change in the plant coverage can be defined by a linear equation. The slope of the lines (S), representative of the sensitivity of the annual thermal loads to plant coverage, vary with the type and age of a building and also with climate. To better understand the heat transfer behavior of the green roofs, monthly averaged diurnal cycle of roof surface temperatures, ceiling heat fluxes, and building cooling demands for the month of July in Phoenix are presented in Fig. 6. In this study, only the summer results are discussed because based on the annual results, cooling loads responded strongly to the increase in plant coverage, while the increase in heating loads did not have so strong response to the plant coverage. In Fig. 6, the simulation

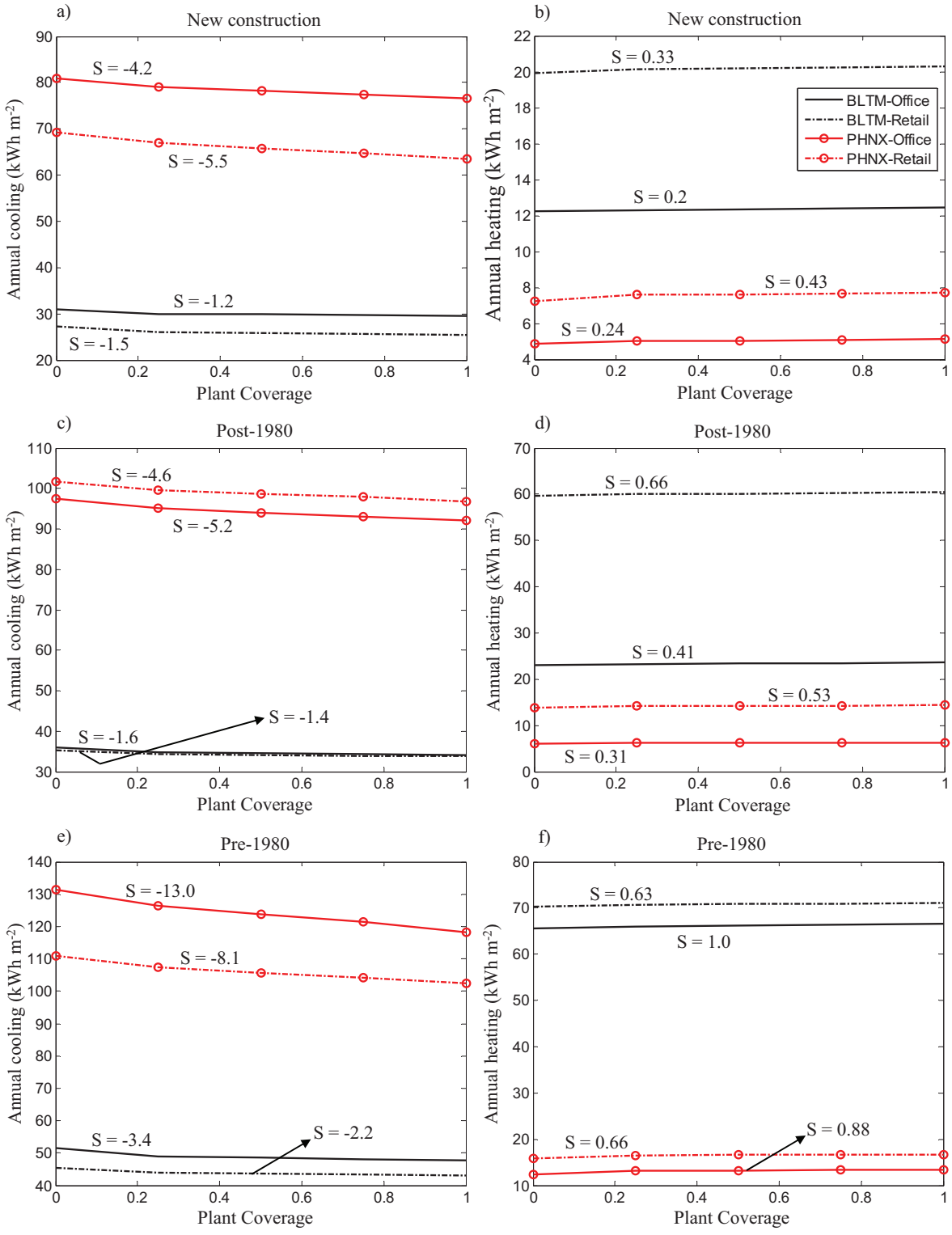

Fig. 5. Annual cooling (left column) and annual heating (right column) loads for the new-construction (a, b), post-1980 (c, d), and pre-1980 (e, f) small office and stand-alone retail buildings in Baltimore, Maryland (black lines) and Phoenix, Arizona (red lines). *S* is the slope for the annual thermal loads with respect to the green roof plant coverage in kWh m^{-2} per plant coverage change from 0 to 1.

results are presented for the small office buildings which in most cases showed the largest cooling load sensitivity to the change in plant coverage. Since the roof assembly of the new-construction and post-1980 office buildings are similar (attic roofs, but with different infiltration rates in the attic zone) their heat transfer processes are comparable. Therefore, here only the monthly averaged results for the new-construction as the less sensitive case are compared against the monthly averaged results for the pre-1980 building as the most sensitive case. These results are for the Phoenix climate that revealed the largest annual cooling demand and sensitivity to the plant coverage. For comparison purposes, the results of the same cases, but with a conventional roof assembly

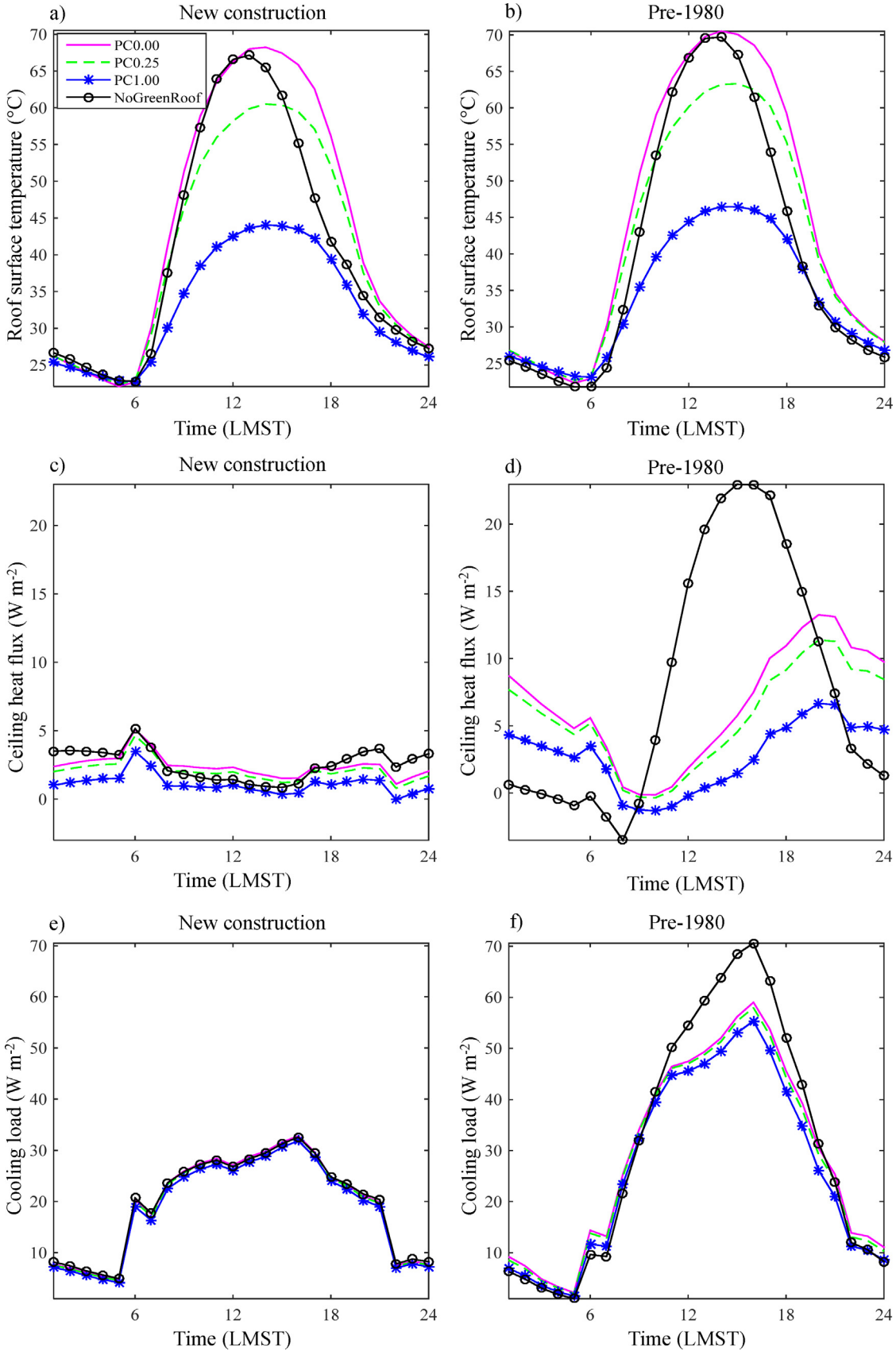

Fig. 6. Comparisons of the monthly averaged roof surface temperatures (a, b), ceiling heat fluxes (c, d), and cooling loads (e, f) for the new-construction (left column) and pre-1980 (right column) small office buildings for the month of July in Phoenix, AZ. Ceiling heat fluxes and cooling loads are in Watt per square meter of floor area.

are also presented in Fig. 6. Since the annual thermal loads demonstrated a linear relation with the plant coverage, only the monthly averaged results of 0.0, 0.25, and 1.0 plant coverage rate simulations are shown in Fig. 6.

The results in Fig. 6 shows that the green roof soil surface temperatures and as a result the amounts of ceiling heat fluxes and cooling loads decrease with increasing plant coverage. The bare-soil roof is the warmest, followed by 25%- and fully-covered green roofs. During the day, there is a small difference between the maximum surface temperature of the bare-soil roof and that of the conventional roof. However, mainly due to the direct exposure to solar radiation, both of these surfaces are significantly warmer than the substrate surface of the fully-covered green roof. The substrate surface temperature difference between the fully-covered and bare-soil roofs is up to 24.3 °C at 1300 LMST*LMST* for the new-construction (Fig. 6a), and 24 °C at 1400 LMST*LMST* for the pre-1980 building (Fig. 6b). These temperature differences tend to diminish at nighttime. At nighttime, due to the longwave radiation trapping between the plant layer and the soil surface, the soil surface lose less heat to the surrounding air and as a result remains relatively warm.

The degree of the influence of green roof plant coverage on the cooling demand of a building depends on the roof contribution in the total building thermal loads. For the new-construction office buildings in Phoenix, a decrease in total daily cooling load in summer from a bare-soil roof to a fully-covered green roof is 4.5%. This amount shows a degree of potential simulation error, if the plant coverage is not considered. This error can reach 8.9% for the pre-1980 office buildings. Unlike the new-construction buildings, in the pre-1980 buildings, due to the weak insulation of the roof assemblies, even a bare-soil green roof significantly affects the amount of cooling demand. The decrease in total daily cooling loads between the conventional roof and the bare-soil roof for the pre-1980 building is 5.8%, whereas this difference in the new-construction is negligible.

4.2.2. *Effects of the building conditions and construction materials*

Roof surface temperatures affect the indoor building climate and energy demand directly through the ceiling heat fluxes and indirectly by modifying the outdoor air temperature. Due to the EnergyPlus limitations, the latter is not considered in this study. The amount of ceiling heat flux itself depends on the construction material and the roof type. The roof type in the DOE new-construction reference small office building is attic roof, while the pre-1980 buildings have flat roofs with insulation above a deck. This difference in roof type explains the different trends in the ceiling heat fluxes of the new-construction and pre-1980 buildings as shown in Fig. 6c and d. The roof type also resulted in the lower peak roof surface temperatures for the new-construction building in Fig. 6a when compared to the peak temperatures for the pre-1980 buildings as shown in Fig. 6b. The lower roof surface temperatures in the new-construction buildings are related to the smaller thermal resistance of the attic roof (consists of two layers including the roof membrane, and metal decking) compared to that of the insulated roof in the pre-1980 buildings (consist of three layers including the roof membrane, IEAD non-residential roof insulation, and metal decking), and larger heat conduction into the attic space.

The large volume of air inside the attic space works as a strong insulator in the new-construction buildings, stronger than the insulation layer in the pre-1980 buildings. As a result, the amount of ceiling heat flux is much smaller in the new-construction building than that in the pre-1980 buildings (Fig. 6c and d). Because of this strong insulator in new-construction, the ceiling heat flux has around a 17 h time lag compared to the roof outside surface temperature, meaning that a change in the roof surface temperature after 1300 LMST*LMST* is affecting the ceiling heat flux after 0600 LMST*LMST*. This time lag for the post-1980 buildings is around 12 h and in the pre-1980 buildings is much shorter being 3 h for the conventional roof and 6 h for the green roofs. Larger roof surface temperatures of green roofs with zero and 25% plant coverage compared to the conventional roof of the new-construction after 1300 LMST*LMST* in Fig. 6a, result in larger amount of the ceiling heat flux between 0600 LMST and 1800 LMST*LMSTLMST* in Fig. 6c (17 h later). Fig. 6a and b show that the green roof has the peak surface temperatures delayed compared to those temperatures for the conventional roof because of the larger thermal inertia due to additional green roof layers. For the same reason, fluctuations of the ceiling heat fluxes are smaller in the presence of a green roof.

As mentioned earlier, roof construction materials are partially responsible for the degree of sensitivity of building types to the change in plant coverage (Fig. 5). For example, the roof insulation of new-construction retail building is thinner than that of the post-1980 retail building (Table 1). As a result, the cooling demand of new-construction retail buildings is more sensitive to the plant coverage.

As shown in Fig. 6c and d, there is a large difference between heat fluxes through the insulated flat roof in the pre-1980 office buildings and the attic roof in the new-construction office buildings. Thermal behavior of these two different types of roofs is very different. Fig. 7 compares the heat gain through the ceiling and the total cooling loads of the new-construction and pre-1980 office buildings with conventional roofs in W m^{-2} of floor area for a typical summer day in Phoenix. Fig. 7 shows that in the new-construction buildings the strong roof insulation creates a significant time lag for the maximum ceiling heat gain. In the new-construction buildings with conventional roof, the maximum ceiling heat gain of 5.2 W m^{-2} occurs at 0600 LMST*LMST*. At the same time, with the zero plant coverage and fully covered green roofs, the maximum ceiling heat gain reduces to 5.1 and 3.5 W m^{-2}, respectively (not shown). In the pre-1980 office buildings with the conventional roof assembly, the maximum ceiling heat gain of 23 W m^{-2} occurs at 1500 LMST*LMST*. This maximum value reduces to 13.2 W m^{-2} at 2000 *LMST* for the bare-soil roof and 6.6 W m^{-2} at 2000 *LMST* for the fully-covered green roof (not shown).

For a typical summer day in the pre-1980 office buildings with the conventional roof, the daily integrated value of ceiling heat gain and cooling loads are 198 Wh m^{-2} and 742 Wh m^{-2} of floor area, respectively. In the new-construction buildings, the daily ceiling heat gain and cooling loads are 62 Wh m^{-2} and 468 Wh m^{-2} of floor area, respectively. This indicates that the contribution of ceiling heat gain in the total daily cooling loads of the pre-1980 office buildings is twice as that in the new-construction (26% versus 13%). Thus, green roofs and their plant coverage are more important and effective in these older office buildings. For the buildings with conventional roofs, Table 4 compares the daily integrated values of ceiling heat gains, cooling loads, and ceiling thermal contributions in the total cooling demands during a typical summer day in Phoenix. This table indicates that the smaller ceiling thermal contributions in the total cooling loads is related to the attic type roofs in the new-construction and post-1980 small office buildings. The larger ceiling contribution in the total daily cooling demand is related to the new-construction stand-alone retail building. Nevertheless, this building has the smallest daily cooling load compared to the other building types. In general, the daily ceiling heat gains, cooling loads, and ceiling thermal contribution in the total building cooling demand are larger for the buildings built before 1980.

4.3. *Comparisons with the 'Ecoroof' model in EnergyPlus*

The present study introduced a new green roof model into EnergyPlus to account for the plant coverage percentage via parallel

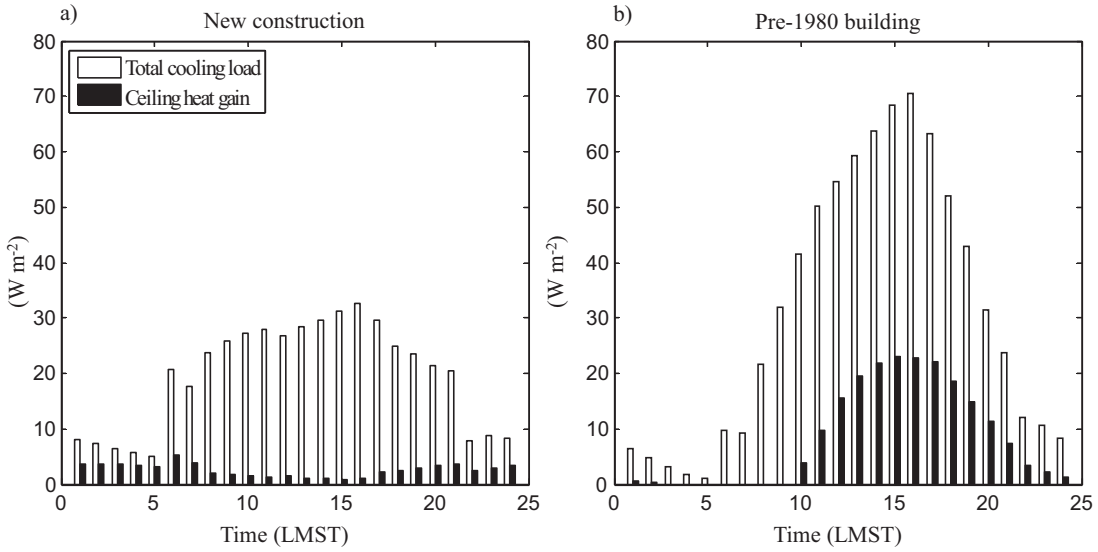

Fig. 7. Hourly comparisons of the ceiling heat gains (black bars) and total cooling loads (white bars) of the (a) new-construction and (b) pre-1980 small office buildings with conventional roofs in W m^{-2} of floor area for a typical summer day (monthly averaged diurnal cycles for the month of July) in Phoenix, AZ.

Table 4
Daily integrated values of ceiling heat gains and cooling loads in Wh m^{-2} of floor area, and percentage of ceiling thermal contributions in the total cooling demands of the buildings with conventional roofs for a typical summer day (monthly averaged diurnal cycle over July) in Phoenix, AZ.

Building type	Ceiling heat gain (Wh m^{-2})	Total cooling loads (Wh m^{-2})	Ceiling thermal contribution in total cooling demand (%)
Office – new const.	62	468	13
Retail – new const.	126	370	34
Office – post-1980	80	569	14
Retail – post-1980	89	549	16
Office – pre-1980	198	742	26
Retail – pre-1980	199	599	33

thermal circuits in the green roof simulations. This model implementation benefited from an existing green roof model, called 'Ecoroof', already available in EnergyPlus [21]. The introduced green roof model has new simulation module for the heat transfer simulations, but it uses the water balance module available in the 'Ecoroof' model. Furthermore, the existing 'Ecoroof' model provides an opportunity to directly compare simulation results of the two models.

For the base-case, simulation results of 'Ecoroof' for a typical summer day in Phoenix, was compared against the results of the new green roof model. The two models are different in their plant and soil sensible and latent heat flux calculations. However, the major difference between the two models is that the 'Ecoroof' model considers fully-covered green roofs, whereas the new green roof model takes the plant coverage into account. As a result, 'Ecoroof' solves energy balance equations for the plants and the soil underneath the plant layer, but the new green roof model solves an additional energy balance equation for the bare portions of green roofs. Therefore, the system of heat transfer equations is different due to different representation of the physical system involving different thermal circuits. Nevertheless, the physical system is the same, so the models should produce similar results under similar physical conditions. The comparison of green roof substrate surface temperature, ceiling heat flux, and building thermal loads showed that the results from the 'Ecoroof' model are similar to those of the 50%-covered green roof model. Since energy modeling of buildings involves many uncertainties with the input parameters, such as the green roof coverage rate, using the 'Ecoroof' model can be considered equivalent to the use of the new green roof model with 50% plant coverage.

5. Conclusions

The temperature of a green roof substrate surface that affects energy use in buildings, primarily depends on the amount of the total radiation absorbed by the surface, the substrate moisture content, and the substrate thermal properties. Despite the fact that these parameters are affected by the amount of plants covering the green roof soil surface, and considering that green roofs are not always fully covered with plants, previous numerical studies simulated fully-covered green roofs. A green roof model that takes into account the plant coverage percentage is implemented into EnergyPlus and validated to investigate the effects of green roof plant coverage on the green roof substrate surface energy balance and building energy consumption. Sensitivity of the results to the local climate, building age, and building type are also investigated. The results show that green roofs have a different thermal performance with different plant coverage, which affect the energy demand in buildings. In general, the green roof substrate surface temperature decreases with an increase in plant coverage predominantly due to the decrease in the amount of received solar radiation at the soil surface as well as the increase in the amount of near surface moisture content and soil surface evaporation. For the base-case simulation, the integrated value of total received

radiation at the bare-soil substrate surface is 32% (6.2 kWh m^{-2}) larger than the total radiation received at the fully-covered green roof soil surface. Additionally, the total daily value of latent heat fluxes over the bare-soil roof is negligible compared to that value over the fully-covered green roof. For the base-case, the daily peak value of the substrate surface temperature for the bare-soil roof is 24 °C (34%) higher than that over the fully-covered green roof. The results of this study also show that for the studied buildings located in climate zones 2 and 4, the annual cooling loads decrease with the increased plant coverage rate. The opposite is true for the heating loads that increase with the increased plant coverage rate. However, in response to the change in plant coverage, the decrease in the annual cooling demand is significantly larger than the increase in the annual heating demand. For example, for the base-case simulation, the annual cooling loads decrease with the rate of 13 kWh m^{-2} of plant coverage area, and the annual heating load increases with the rate of 0.88 kWh m^{-2} of plant coverage area.

The results show that for a weak insulation of a roof on the pre-1980 office buildings, the maximum surface temperature of the fully-covered green roof is 34% cooler than that of the bare-soil roof in a typical summer day in Phoenix. This temperature difference results in 5% decrease of the building cooling demand during that time period. In this study, the green roof plant coverage effects on the building cooling demand were only accounted by roof/ceiling conduction heat transfer, so the cooling effects of green roofs on the outdoor air temperature is not considered in the simulations. Green roofs, considered as one of the effective urban heat island mitigations, affect the outdoor air temperature through convective heat transfer. In addition, in response to the reduction in building energy use, the amount of discharged anthropogenic heat flux into outdoor air decreases. These effects, and a dynamic simulation of outdoor air temperature are not included in EnergyPlus. Despite the fact that the immediate effects of green roofs on building energy use through conductive heat fluxes are more effective than their convective indirect effects, it is anticipated that in the presence of a dynamic air temperature simulation, green roofs, and thus their plant coverage, affect the indoor environment and building energy demand more effectively. The importance of this factor is expected to be larger in urban areas with a larger surface areas covered by green roofs. It is desirable to consider these effects in future studies.

Acknowledgments

This study is sponsored by the EFRI-1038264/EFRI-1452045 award from the National Science Foundation (NSF), Division of Emerging Frontiers in Research and Innovation (EFRI). In addition, authors would like to thank Prof. Paulo Tabares-Velasco at the Colorado School of Mines for his valuable inputs.

Appendix.

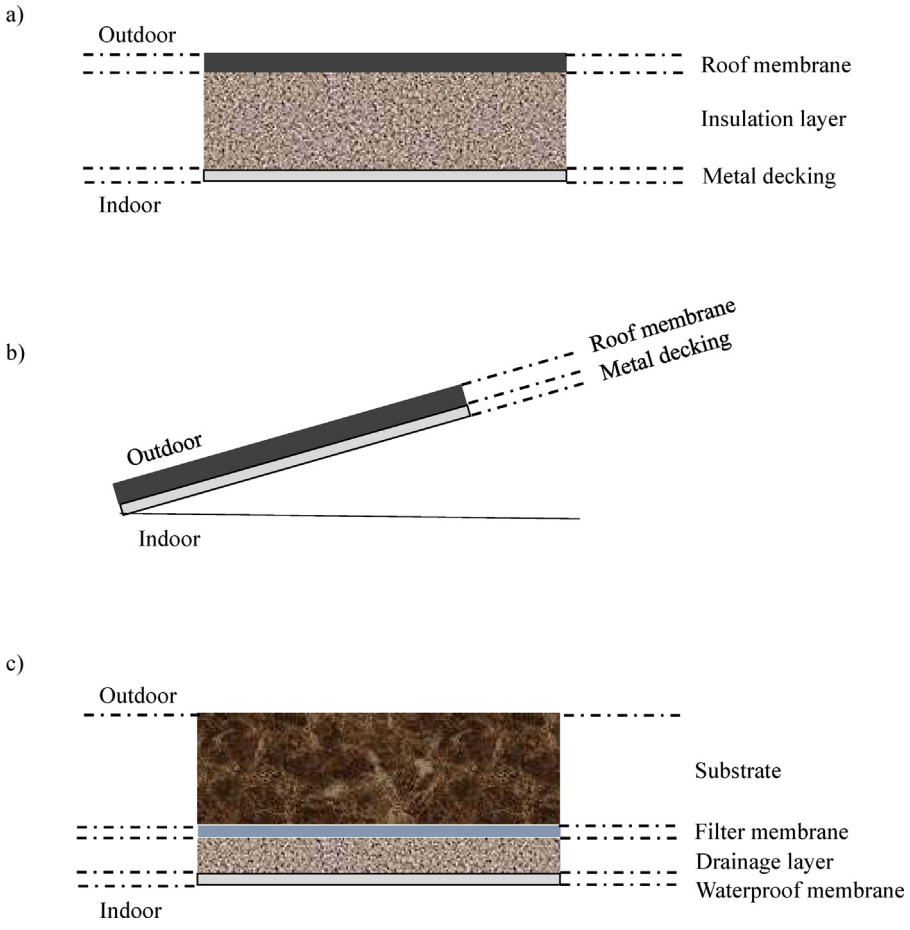

Fig. A1. Sketch of the layers of the (a) IEAD non-residential, (b) attic non-residential, and (c) green roofs that are used in the simulations. Thicknesses of the layers are not scaled in the figure. Thicknesses and physical characteristics of the material layers are provided in Tables 1 and 2.

References

[1] W.G. Hansen, How accessibility shapes land use, J. Am. Inst. Plan. 25 (1959) 73–76.
[2] S.J. Stankowski, Population density as an indirect indicator of urban and suburban land–surface modifications, US Geol. Surv. Prof. Pap. 800 (1972) 219–224.
[3] H. Akbari, L. Shea Rose, H. Taha, Analyzing the land cover of an urban environment using high-resolution orthophotos, Landsc. Urban Plan. 63 (2003) 1–14.
[4] U. Berardi, A. GhaffarianHoseini, A. GhaffarianHoseini, State-of-the-art analysis of the environmental benefits of green roofs, Appl. Energy 115 (2014) 411–428.
[5] J. Mentens, D. Raes, M. Hermy, Green roofs as a tool for solving the rainwater runoff problem in the urbanized 21st century? Landsc. Urban Plan. 77 (2006) 217–226.
[6] V. Stovin, N. Dunnett, A. Hallam, Green roofs – getting sustainable drainage off the ground, in: 6th International Conference of Sustainable Techniques and Strategies in Urban Water Management, 2007, pp. 11–18.
[7] N.H. Wong, Y. Chen, C.L. Ong, A. Sia, Investigation of thermal benefits of rooftop garden in the tropical environment, Build. Environ. 38 (2003) 261–270.
[8] H. Takebayashi, M. Moriyama, Surface heat budget on green roof and high reflection roof for mitigation of urban heat island, Build. Environ. 42 (2007) 2971–2979.
[9] K. Liu, B. Bass, Performance of Green Roof Systems, National Research Council Publications Archive, Canada, 2005, NRCC-47705.
[10] M. Zhao, P.C. Tabares-Velasco, J. Srebric, S. Komarneni, Comparison of green roof plants and substrates based on simulated green roof thermal performance with measured material properties, in: 13th Conference of International Building Performance Simulation Association, Chambéry, France, August 26–28, 2013.
[11] G. Virk, A. Jansz, A. Mavrogianni, A. Mylona, J. Stocker, M. Davies, The effectiveness of retrofitted green and cool roofs at reducing overheating in a naturally ventilated office in London: direct and indirect effects in current and future climates, Indoor Built Environ. 23 (2014) 504–520.
[12] J.C. Berndtsson, L. Bengtsson, K. Jinno, Runoff water quality from intensive and extensive vegetated roofs, Ecol. Eng. 35 (2009) 369–380.
[13] J. Yang, Q. Yu, P. Gong, Quantifying air pollution removal by green roofs in Chicago, Atmos. Environ. 42 (2008) 7266–7273.
[14] P.C. Tabares-Velasco, J. Srebric, A heat transfer model for assessment of plant based roofing systems in summer conditions, Build. Environ. 49 (2012) 310–323.
[15] D. Li, E. Bou-Zeid, M. Oppenheimer, The effectiveness of cool and green roofs as urban heat island mitigation strategies, Environ. Res. Lett. 9 (2014) 055002.
[16] S. Ouldboukhitine, R. Belarbi, D.J. Sailor, Experimental and numerical investigation of urban street canyons to evaluate the impact of green roof inside and outside buildings, Appl. Energy 114 (2014) 273–282.
[17] M.J. Clark, Y. Zheng, Fertilizer rate and type affect sedum-vegetated green roof mat plant performance and leachate nutrient content, HortScience 49 (2014) 328–335.
[18] E.P.D. Barrio, Analysis of the green roofs cooling potential in buildings, Energy Build. 27 (1998) 179–193.
[19] T.G. Theodosiou, Summer period analysis of the performance of a planted roof as a passive cooling technique, Energy Build. 35 (2003) 909–917.
[20] D.J. Sailor, A green roof model for building energy simulation programs, Energy Build. 40 (2008) 1466–1478.
[21] The U.S. Department of Energy (DOE), EnergyPlus Energy Simulation Software (http://apps1.eere.energy.gov/buildings/energyplus/energyplus_about.cfm).
[22] P.C. Tabares-Velasco, J. Srebric, Experimental quantification of heat and mass transfer process through vegetated roof samples in a new laboratory setup, Int. J. Heat Mass Transfer 54 (2011) 5149–5162.
[23] P.C. Tabares-Velasco, M. Zhao, N. Peterson, J. Srebric, R. Berghage, Validation of predictive heat and mass transfer green roof model with extensive green roof field data, Ecol. Eng. 47 (2012) 165–173.
[24] D.B. Crawley, J.W. Hand, M. Kummert, B.T. Griffith, Contrasting the capabilities of building energy performance simulation programs, Build. Environ. 43 (2008) 661–673.
[25] DOE, Getting started with EnergyPlus – Basic Concepts Manual – Essential Information You Need about Running EnergyPlus, U.S. Department of Energy, 2013.
[26] N. Yaghoobian, P.C. Tabares-Velasco, M. Heidarinejad, J. Srebric, Green Roof Model with Plant Coverage Rate, U.S. Department of Energy, EnergyPlus Engineering Reference, and EnergyPlus Input Output Reference, 2015.
[27] M. Zhao, P.C. Tabares-Velasco, J. Srebric, S. Komarneni, R. Berghage, Effects of plant and substrate selection on thermal performance of green roofs during the summer, Build. Environ. 78 (2014) 199–211.
[28] National Renewable Energy Laboratory (NREL), National Solar Radiation Data Base; 1961–1990: Typical Meteorological Year 2 (http://rredc.nrel.gov/solar/old_data/nsrdb/1961-1990/tmy2/).
[29] M. Deru, K. Field, D. Studer, K. Benne, B. Griffith, P. Torcellini, B. Liu, M. Halverson, D. Winiarski, M. Rosenberg, U.S. Department of Energy Commercial Reference Building Models of the National Building Stock, 2011.
[30] Pacific Northwest National Laboratory, Advanced Energy Retrofit Guide, Retail Buildings, 2011.
[31] A. Niachou, K. Papakonstantinou, M. Santamouris, A. Tsangrassoulis, G. Mihalakakou, Analysis of the green roof thermal properties and investigation of its energy performance, Energy Build. 33 (2001) 719–729.
[32] H. Castleton, V. Stovin, S. Beck, J. Davison, Green roofs; building energy savings and the potential for retrofit, Energy Build. 42 (2010) 1582–1591.
[33] I. Jaffal, S. Ouldboukhitine, R. Belarbi, A comprehensive study of the impact of green roofs on building energy performance, Renew. Energy 43 (2012) 157–164.
[34] The U.S. Department of Energy (DOE), Commercial Reference Buildings (http://energy.gov/eere/buildings/commercial-reference-buildings).
[35] Energy Standard for Buildings Except Low-Rise Residential Buildings, in: ASHRAE (Ed.), ANSI/ASHRAE/IESNA Standard 90.1-2004, American Society of Heating, Refrigerating and Air-Conditioning Engineers, Atlanta, GA, 2004.
[36] ASHRAE (Ed.), Energy Efficient Design of New Buildings Except Low-Rise Residential Buildings. ANSI/ASHRAE/IESNA Standard 90.1-1989, American Society of Heating, Refrigerating and Air-Conditioning Engineers, Atlanta, GA, 1989.
[37] M. Lewin, E.M. Pearce (Eds.), Handbook of Fiber Chemistry, 2nd ed. (revised and expanded), CRC Press, 1998.
[38] A. Lyons, Materials for Architects and Builders, 4th ed., Elsevier Ltd., 2010.
[39] W.V. Titow (Ed.), PVC Technology, 4th ed., Elsevier Applied Science Publishers, New York, USA, 1984.
[40] ASM International, Characterization and Failure Analysis of Plastics, Library of Congress Cataloging-in-Publication Data, United States of America, 2003.
[41] P. Tabares-Velasco, J. Srebrić, The role of plants in the reduction of heat flux through green roofs: laboratory experiments, Klim. grej. hlađ. 38 (2009) 55–62.